# Temperature-Dependent Atomic Models of Detergent Micelles Refined against Small-Angle X-Ray Scattering Data

*Miloš T. Ivanović, Linda K. Bruetzel, Jan Lipfert,* and Jochen S. Hub**

***Abstract:*** *Surfactants have found a wide range of industrial and scientific applications. In particular, detergent micelles are used as lipid membrane mimics to solubilize membrane proteins for functional and structural characterization. However, an atomic-level understanding of surfactants remains limited because many experiments provide only low-resolution structural information on surfactant aggregates. In this work, small-angle X-ray scattering is combined with molecular dynamics simulations to derive fully atomic models of two maltoside micelles at temperatures between 10 °C and 70 °C. The micelles take the shape of general tri-axial ellipsoids and decrease in size and aggregation number with increasing temperature. Density profiles of hydrophobic groups and water along the three principal axes reveal that the minor micelle axis closely mimics lipid membranes. The results suggest that coupling atomic simulations with low-resolution data allows the structural characterization of surfactant aggregates.*

As fundamental building blocks of soft-matter systems, surfactants (surface-active agents) have found a wide range of industrial, scientific, and consumer applications.[1,2] For instance, surfactants and their micellar aggregates may accelerate or inhibit chemical reactions as compared to an aqueous medium.[3,4] Since surfactants may alter their structure in response to external stimuli,[5] they have been used as a carrier for therapeutic molecules, to build confined reaction platforms for sustainable chemistry, and for modifying the characteristics of food products.[6–8] Surfactants are routinely applied in cosmetics, personal care, and cleaning products, and the world market of surfactants was valued at about 30 billion US dollars in 2015.[9] Beside such applications, surfactants serve as model systems in soft matter research, as their self-organization into structures such as micelles or bilayers is still not fully understood.[2] A functional understanding of such soft matter systems remains limited, which is partly due to the lack of reliable atomic models.

Detergents are the most widely used type of surfactants. Above the critical micelle concentration (CMC), detergent monomers in solution self-assemble and form micelles of various shapes such as spheres, ellipsoids or cylinders. The formation of micelles involves a delicate balance of free-energy contributions from enthalpy and both solute and solvent entropy.[10,11] Consequently, many fundamental properties of micelles, such as the CMC, the aggregation number $N$, and their size and shape are temperature-dependent.[12]

Since the cross-section of certain detergent micelles resembles lipid membranes, micelles are frequently used as membrane mimics to solubilize membrane proteins for biochemical and structural characterization.[13] In experiments, protein–detergent complexes are often exposed to varying temperatures, for instance in NMR studies to accelerate diffusion and hence to improve the quality of spectra, or to dissect thermodynamic equilibria involving conformational changes or ligand binding.[14,15] Choosing a suitable detergent for membrane protein solubilization is often accomplished by trial and error; however, recent work suggests that matching of the hydrophobic thickness between the micelle and the membrane protein of interest can provide a route towards rational selection and design of detergent micelles.[16,17] Hence, accurate information on the shape and size of detergent micelles, also as function of temperature, represents a starting point to improve the stability of protein–detergent complexes.

Detergent micelles have been studied using a range of methods, including small-angle X-ray and neutron scattering (SAXS/SANS),[18–21] NMR self-diffusion,[22] and several others.[23–25] The information content of such data is often insufficient to derive atomic models of micelles. Complementary, molecular dynamics (MD) simulations have been used to gain atomic insight into micelles;[26–29] however, it remains unclear to which extent force field imperfections bias the structure and shape of the simulated micelle.[30] Hence, methods that integrate experimental data into MD simulations are needed to obtain reliable atomic models of micelles.

Herein, we derived atomic models of two maltoside micelles, n-dodecyl-β-D-maltoside (DDM) and n-decyl-β-D-maltoside (DM; Figure 1) at temperatures between 10 °C and 70 °C, by combining experimental SAXS data with all-atom MD simulations. The data were collected at beam line 12ID of the Advanced Photon Source[31] (Supporting Information, Methods). We incorporated the SAXS data as an energetic restraint into MD simulations, allowing us to refine micellar models against scattering data. Because all SAXS predictions were based on explicit-solvent models, the calculations

[*] M. T. Ivanović, J. S. Hub
Institute for Microbiology and Genetics, Georg-August-University Göttingen
Justus-von-Liebig Weg 11, 37077 Göttingen (Germany)
E-mail: jochen.hub@physik.uni-saarland.de
L. K. Bruetzel, J. Lipfert
Department of Physics and Center for Nanoscience, LMU Munich
Amalienstrasse 54, 80799 Munich (Germany)
E-mail: Jan.Lipfert@lmu.de
J. S. Hub
Current address: Saarland University, Theoretical Physics
Campus E2 6, 66123 Saarbrücken (Germany)
Supporting information and the ORCID identification number(s) for the author(s) of this article can be found under: https://doi.org/10.1002/anie.201713303.

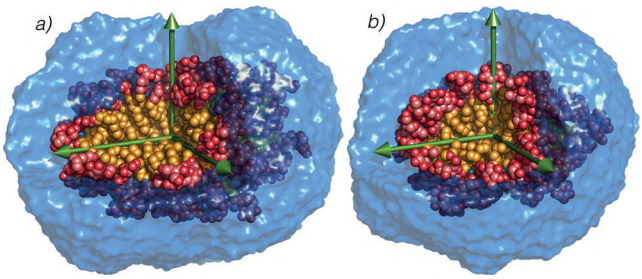


***Figure 1.*** Atomic models of a) DDM and b) DM micelles at 25 °C, refined against experimental SAXS data. Red spheres: head groups; orange spheres: tails; blue surface: explicit water included into the calculations of SAXS profiles. Green arrows indicate principal axes (length 4 nm).

involve accurate physical models for the hydration layer and the excluded solvent, thereby avoiding any solvent-related fitting parameters and, in turn, enabling highly predictive structural modeling.[32]

We determined the aggregation number $N_{agg}$ (that is, the number of detergent monomers per micelle) as function of temperature from the experimental SAXS data using two independent methods. First, we determined $N_{agg}$ from the extrapolated forward scattering intensity $I_0$, obtained by Guinier analysis of the data in the low $q$-region (Supporting Information, Figure S1), together with the expected scattering intensity from a detergent monomer. This approach is model-free in the sense that it does not rely on a particular representation of micelle structure, and it has been successfully applied to a range of different detergent micelles at room temperature.[20,21] Here, we measured and explicitly took into account the temperature dependencies of the buffer and detergent densities (Supporting Information, Methods and Figures S2–S4). The data show that $N_{agg}$ decreases with increasing temperature (Figure 2, red triangles), by about 20 % going from 10 °C to 70 °C.

Second, we estimated the experimental $N_{agg}$ using a series of free MD simulations with increasing $N_{agg}$ at each temperature. From each simulation, we computed the scattering profile and compared the position of the pronounced minimum at $q \approx 1$ nm$^{-1}$ to the experimental data to determine the best fitting simulations and thus the estimated experimental $N_{agg}$ (Figure 2, black circles; Supporting Information, Methods and Figures S5, S6).

The two approaches to determining $N_{agg}$ give good agreement both for the absolute values and for the temperature dependencies; for DM, the agreement is even excellent and within experimental error. For DDM, some deviations are apparent, in particular at the highest temperature. These deviations might stem from the fact that the lower density for DDM compared to DM makes the analysis more sensitive to uncertainties in the temperature dependence of the detergent density, both for estimates from $I_0$ and from MD simulations. Notably, our $N_{agg}$ estimates for 25 °C agree with previous reports.[18,20,21]

Having determined the temperature dependence of $N_{agg}$ enables us to test the analytic model for micellar aggregation proposed by Chandler and co-workers.[11] Using plausible

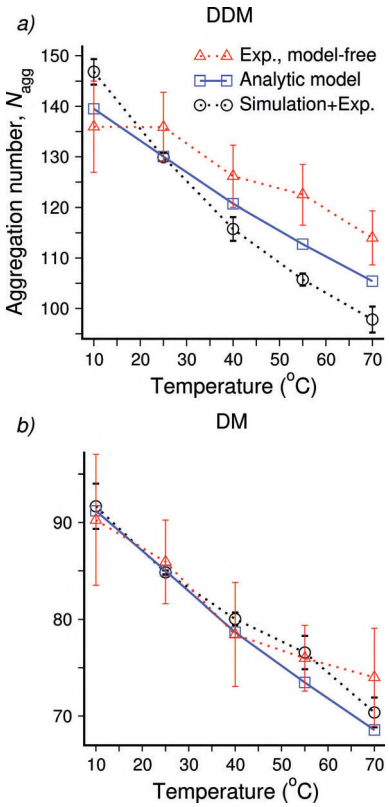


***Figure 2.*** Aggregation number of DDM and DM micelles versus temperature, derived from SAXS data in a model-free procedure (red), from SAXS and MD simulations (black), and from an analytical model.[11] Error bars denote 1 SEM. Error bars on red symbols were obtained from repeated measurements and taking into account a 5 % uncertainty in the intensity calibration. Error bars on black symbols were obtained from error propagation (see the Supporting Information, Methods).

values for the alkyl chain-length parameter (Supporting Information, Methods), the Chandler model (Figure 2, blue line and symbols) provides a good description of the experimental data. The remaining discrepancy can be explained by the fact that Chandler's theory assumes a spherical micelle, whereas DDM micelles and, to a lower degree, DM micelles take an ellipsoidal shape (see below).

The scattering profiles computed from 50 ns of free MD simulations of DM and DDM micelles at the temperatures between 10 °C and 70 °C conducted at the estimated $N_{agg}$ (Figure 2) give reasonable, but not perfect agreement with the experimental data (Figure 3, blue and red curves, respectively). The experimental data suggest that the micelles under our conditions are monodisperse (see the Supporting Information, text), making it unlikely that heterogeneous ensembles over different $N_{agg}$, that is, polydispersity in micelle size, accounts for the remaining residuals. Furthermore, we found that modeling polydispersity in $N_{agg}$ hardly improved the agreement (Supporting Information, Figure S9), indicating that not a distribution over $N_{agg}$, but instead incorrect micellar shapes account for the residuals between simulation and experiment. Specifically, the overpronounced minima ($q \approx 1$ nm$^{-1}$) and maxima ($q \approx 2$ nm$^{-1}$) in the calculated profiles

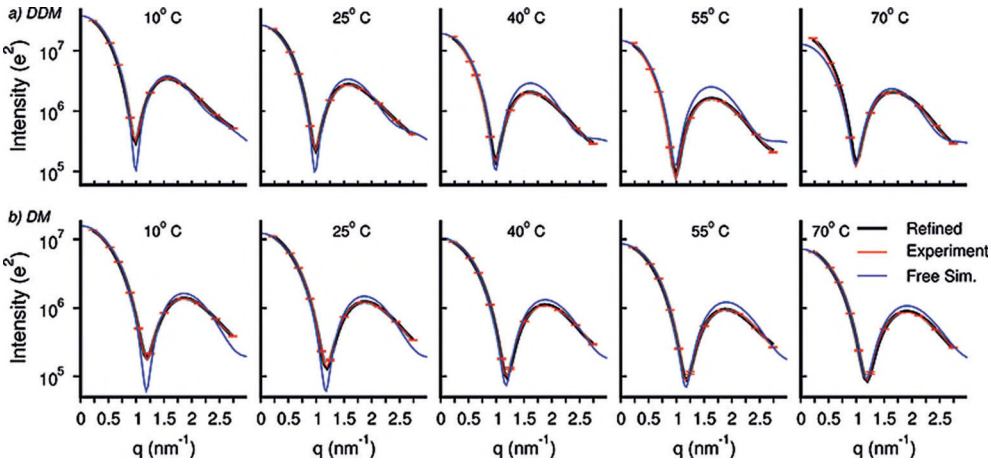


***Figure 3.*** Experimental SAXS curves (red, representative errors obtained from repeated measurements) computed from free (blue) and refined simulations (black) of DDM (top row) and DM (bottom row) micelles at different temperatures as indicated in the subplots.

suggest that micelles in free simulations were slightly too spherical, which is likely a consequence of small imperfections of the CHARMM36 force field[33] used in our simulations.

To refine the micelles against the experimental SAXS data, we introduced the experimental curves as an energetic restraint into the simulations.[34] Ultraweak restraints of 2–3 kJ mol$^{-1}$ for the entire system (Supporting Information, Figure S7) were sufficient to restrain the micelles to shapes in quantitative agreement with the data (Figure 3, red and black curves). We found that the SAXS-derived restraints hardly influenced the distribution of tail length as compared to free simulations (Supporting Information, Figures S10, S11), but the restraints modified the shape of the micelle, as apparent from the distributions of radii of gyration around the three principal axes (Supporting Information, Figure S14). Representative snapshots of refined DDM and DM micelles at 25 °C shown in Figure 1 reveal slightly elongated ellipsoidal shapes.

To characterize the refined micellar shapes more quantitatively, we computed the density profiles along the three principal axes, decomposed into contributions from the hydrophobic tails, head groups, and water (Figure 4 b–g). The density profiles were computed from 300 ns of SAXS-restraint simulations at 25 °C, and from 40–60 ns for all other temperatures, suggesting that conformational fluctuations of the micelles, to the extent allowed by the SAXS restraints, are included in the density profiles. As evident from the three distinct semi-axes, the micelles did not take the shape of a spheroid (an ellipsoid with two identical semi-axes), but instead took the shape of a general tri-axial ellipsoid. Figure 4 h/i summarizes the semi-axes for temperatures between 10 °C and 70 °C, taken from the density of tails and head groups. The micelles shrink with increasing temperatures along the major and middle axes, as expected from the decreasing $N_{agg}$. The overall micelle dimensions shrink by reducing the thickness of the hydrophobic region and not by reducing the thickness of the head group region (Supporting Information, Figures S12 and S13). In contrast, the extension along the minor axis is nearly temperature-invariant, likely because the shortest axis is constrained by the extensions of the detergent tails, which are almost independent of temperature (Supporting Information, Figure S12). Further, along all three axes, the water density decays gradually over a range of about 1.5 nm between the bulk and hydrophobic tail regions (Figure 4 b–g, cyan), similar to the water density detected by neutron reflectometry for phosphatidylcholine membranes.[35]

For both DDM and DM at most temperatures, the micelles are mainly characterized by one long and two approximately equal shorter semi-axes (Figure 4 h,i; Supporting Information, Figures S12, S14), that is, the micelles rather resemble prolate than oblate ellipsoids; DDM micelles at 55 °C and 70 °C even take on close to ideal prolate shapes. This finding seems to contrast previous fits of an implicit two-component micelle model to SAXS data, deserving further explanation. Previously, micellar shapes were extracted from SAXS data by fitting symmetrized geometric models, namely prolate or oblate ellipsoids with only two independent semi-axes (Figure 4 a with $a = b$ and $t_a = t_b = t_c$).[20,21] Such fits, however, may become bistable, thereby yielding prolate and oblate models with similar agreement with the data. In case of bistable fits, the physically relevant solution was chosen such that the short semi-axis is shorter than the detergent chain, thereby avoiding a vacuum cavity in the micelle.[10] For DDM and DM, this procedure has led to the proposition of oblate micellar shapes.[20] By contrast, for the present study, we avoided any assumptions about the symmetry, but we let the simulation decide which micellar shape is most plausible in the light of the data and the force field. Thereby, we obtained qualitatively different, namely more elongated prolate-like micellar shapes.

Recent work suggested that the stability of a protein-detergent complex improves if the hydrophobic thickness matches between micelle and protein.[16,17] To test if the refined DDM and DM micelles provide an accurate mimic for lipid membranes, we compared the hydrophobic and the polar profiles along the three principal axes with the profiles of two typical model membranes, composed of either palmitoyl oleoyl phosphatidylcholine (POPC) or of dimyristoyl phosphatidylcholine (DMPC). For the density of water as well as for the hydrophobic tails, we found an excellent match between the minor axis of the micelles and the lipid membranes, in particular between DDM and POPC on the one hand, and between DM and DMPC on the other hand (Figure 5 e,f). In contrast, the profiles along the middle and major axes are too wide to match the lipid membranes (Figure 5 a–d). This suggests that membrane proteins are

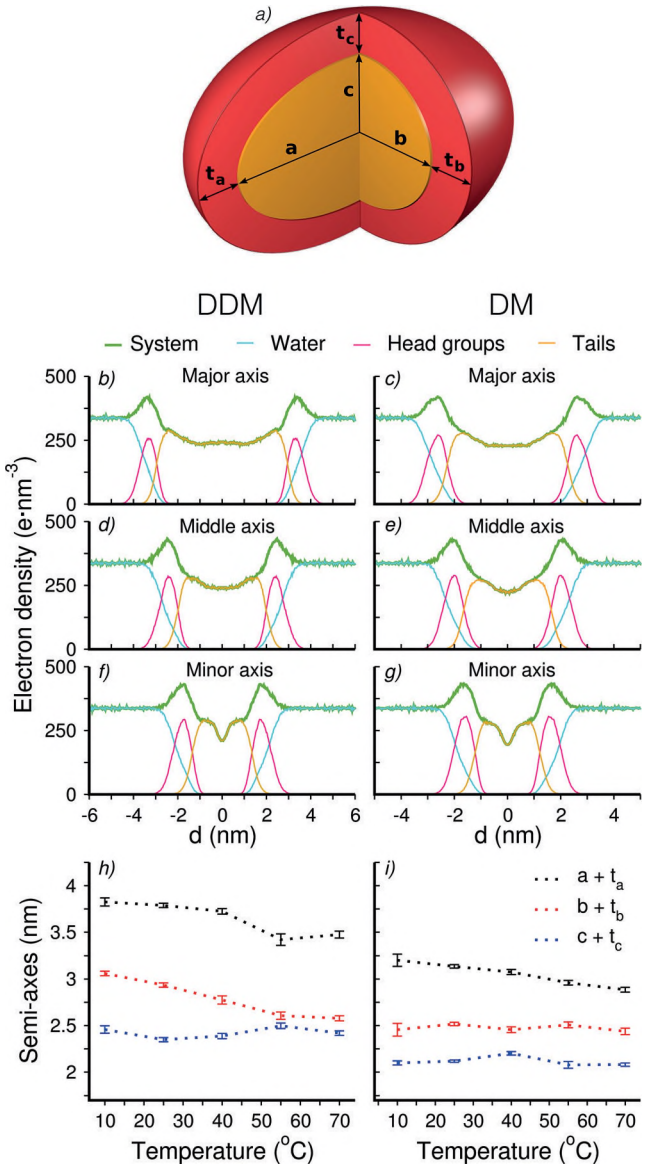


***Figure 4.*** a) Representation of a micelle as a two-component tri-axial ellipsoid. Orange: detergent tails; red: head groups. b)–g) Density profiles along the major, middle, and minor principal axes of refined DDM (b, d, f) and DM (c, e, g) micelles at 25 °C. h), i) Semi-axes of DDM and DM micelles versus temperature, defined as FWHM of the densities (Supporting Information, Methods). Hydrophobic semi-axes *a*, *b*, *c* (Supporting Information, Figure S12) and head group thicknesses $t_a$, $t_b$, $t_c$ are illustrated in (a). Error bars denote 1 SEM obtained from block averaging.

predominantly embedded into DDM and DM micelles such that the membrane-normal axis of the protein is aligned along the minor micelle axis. Furthermore, since maltosides have been frequently used to solubilize membrane proteins, our analysis supports the view that a match between the minor micelle axis and the lipid membrane is the key determinant for successful protein solubilization.[16]

To conclude, we have derived fluctuating atomic models of two maltoside micelles by combining experimental SAXS data with MD simulations and explicit-solvent SAXS predictions. Free simulations revealed reasonable, but not quantitative agreement with experimental SAXS curves; hence a weak experiment-derived energetic bias was required to obtain simulations that accurately agree with experimental conditions. We found that DDM and DM micelles take the shape of a general tri-axial ellipsoid, where major and middle axes decreased with increasing temperature, whereas the minor axis was approximately constant between 10 °C and 70 °C. Density profiles along the principal axes showed that the cross-section along the minor axis of the micelles closely mimics lipid membranes, with implications on the rational design of stable protein–detergent complexes. We found the aggregation number $N_{agg}$ to decrease moderately with increasing temperature, predominantly by shrinking the major and middle axis of the micelle.

The study highlights that a direct coupling between experiment and simulation provides more spatially detailed and more reliable structures of soft matter systems, as compared to each of the methods alone. Specifically, SAXS provides information on the overall shape and size, but does not provide information at the atomic level. MD simulations provide atomic details with reasonably accurate potential energy functions (force fields), and they naturally account for thermal fluctuations; however, MD simulations have difficulties with obtaining large-scale features a priori. As such, SAXS and MD provide highly complementary physicochemical information. Our work may provide a starting point for a rational selection of detergents for solubilizing membrane proteins, and for further improvements of detergent force fields. The fact that the minor axes are approximately independent of temperature (Figure 4) implies that a match between the length of the hydrophobic part of the protein and the micelle thickness would be maintained over a significant temperature range and, consequently, that the maltosides investigated here can be used for solubilization over a range of temperatures. Future work will have to test to what extent these trends also hold for other detergents. While the refinement of DM and DDM micelles was simplified by their monodispersity in size, the refinement of highly polydisperse micelle solutions will likely require the explicit treatment of heterogeneous ensembles. Furthermore, we are currently extending the procedure for incorporating complementary SANS data, providing a framework for integrative structural modeling of soft-matter systems.

## Acknowledgements

We thank Linda Columbus and Sebastian Doniach for discussions, Linda Columbus for providing detergent samples, Sönke Seifert for help with measurements at beam line 12ID at the Advanced Photon Source, and Annalena Salditt for performing the density measurements. We thank Roman Shevchuk for support with SAXS calculations. We acknowledge funding from the Deutsche Forschungsgemeinschaft (HU 1971/1-1, HU 1971/1-3, HU 1971/1-4, Nanosystems Initiative Munich). This research used resources of the Advanced Photon Source, a U.S. Department of Energy (DOE) Office of Science User Facility operated for the DOE

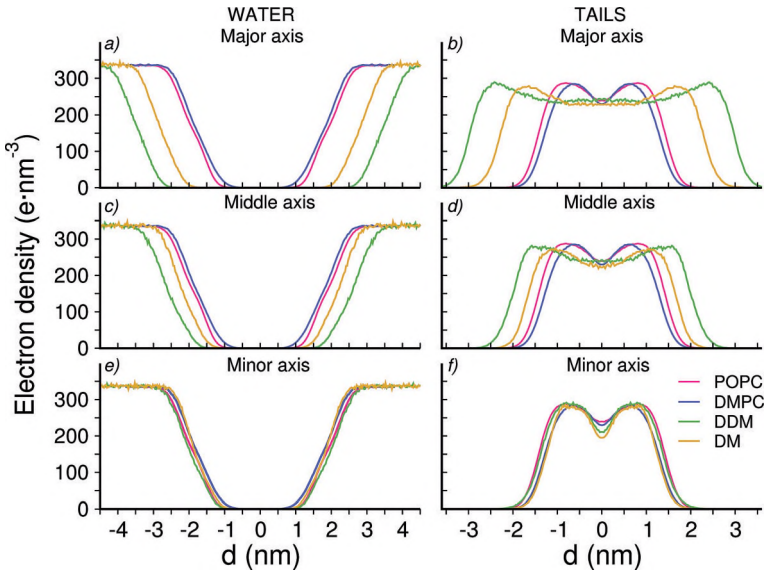


***Figure 5.*** Density profiles at 25 °C of water (left column) and hydrophobic detergent tails (right column) along the major axis (a,b), middle axis (c,d), and minor axis (e,f) of micelles of DDM (green lines) and DM (dark yellow lines). For comparison, density profiles of water and hydrophobic tails across lipid membranes of POPC (red lines) and DMPC (blue lines) are shown.

Office of Science by Argonne National Laboratory under Contract No. DE-AC02-06CH11357.

## *Conflict of interest*

The authors declare no conflict of interest.

**Keywords:** detergent micelles · molecular dynamics · SAXS · structure refinement

**How to cite:** *Angew. Chem. Int. Ed.* **2018**, *57*, 5635–5639
*Angew. Chem.* **2018**, *130*, 5737–5741

[1] S. Jain, F. S. Bates, *Science* **2003**, *300*, 460–464.
[2] M. J. Rosen, J. T. Kunjappu, *Surfactants and interfacial phenomena*, Wiley, Chichester, **2012**.
[3] T. Dwars, E. Paetzold, G. Oehme, *Angew. Chem. Int. Ed.* **2005**, *44*, 7174–7199; *Angew. Chem.* **2005**, *117*, 7338–7364.
[4] T. Dwars, E. Paetzold, G. Oehme, *Angew. Chem.* **2005**, *117*, 7338–7364.
[5] A. Patist, J. R. Kanicky, P. K. Shukla, D. O. Shah, *J. Colloid Interface Sci.* **2002**, *245*, 1–15.
[6] Y. Geng, P. Dalhaimer, S. Cai, R. Tsai, M. Tewari, T. Minko, D. E. Discher, *Nat. Nanotechnol.* **2007**, *2*, 249–255.
[7] S. Diodati, P. Dolcet, M. Casarin, S. Gross, *Chem. Rev.* **2015**, *115*, 11449–11502.
[8] D. Balzer, H. Luders, *Nonionic surfactants: Alkyl polyglucosides, Vol. 91*, CRC, Boca Raton, **2000**.
[9] *Global Surfactant Market, 4th ed.*, Acmite Market Intelligence, **2016**.
[10] C. Tanford, *The Hydrophobic Effect: Formation of Micelles and Biological Membranes, 2nd ed.*, Wiley, Chichester **1980**.
[11] L. Maibaum, A. R. Dinner, D. Chandler, *J. Phys. Chem. B* **2004**, *108*, 6778–6781.
[12] M. G. D'Andrea, C. C. Domingues, S. V. Malheiros, F. G. Neto, L. R. Barbosa, R. Itri, F. C. Almeida, E. de Paula, M. L. Bianconi, *Langmuir* **2011**, *27*, 8248–8256.
[13] A. M. Seddon, P. Curnow, P. J. Booth, *Biochim. Biophys. Acta Biomembr.* **2004**, *1666*, 105–117.
[14] R. Horst, A. L. Horwich, K. Wüthrich, *J. Am. Chem. Soc.* **2011**, *133*, 16354–16357.
[15] T. H. Kim, K. Y. Chung, A. Manglik, A. L. Hansen, R. O. Dror, T. J. Mildorf, D. E. Shaw, B. K. Kobilka, R. S. Prosser, *J. Am. Chem. Soc.* **2013**, *135*, 9465.
[16] L. Columbus, J. Lipfert, K. Jambunathan, D. A. Fox, A. Y. Sim, S. Doniach, S. A. Lesley, *J. Am. Chem. Soc.* **2009**, *131*, 7320.
[17] M. A. O'Malley, M. E. Helgeson, N. J. Wagner, A. S. Robinson, *Biophys. J.* **2011**, *101*, 1938–1948.
[18] C. Dupuy, X. Auvray, C. Petipas, I. Rico-Lattes, A. Lattes, *Langmuir* **1997**, *13*, 3965–3967.
[19] J. B. Hayter, T. Zemb, *Chem. Phys. Lett.* **1982**, *93*, 91–94.
[20] J. Lipfert, L. Columbus, V. B. Chu, S. A. Lesley, S. Doniach, *J. Phys. Chem. B* **2007**, *111*, 12427–12438.
[21] R. C. Oliver, J. Lipfert, D. A. Fox, R. H. Lo, S. Doniach, L. Columbus, *PLoS One* **2013**, *8*, e62488.
[22] F. Nilsson, O. Söderman, P. Hansson, I. Johansson, *Langmuir* **1998**, *14*, 4050–4058.
[23] R. Hargreaves, D. T. Bowron, K. Edler, *J. Am. Chem. Soc.* **2011**, *133*, 16524–16536.
[24] K. Kameyama, T. Takagi, *J. Colloid Interface Sci.* **1990**, *137*, 1–10.
[25] C. La Mesa, A. Bonincontro, B. Sesta, *Colloid Polym. Sci.* **1993**, *271*, 1165–1171.
[26] K. Watanabe, M. Ferrario, M. L. Klein, *J. Phys. Chem.* **1988**, *92*, 819–821.
[27] D. Tieleman, D. Van der Spoel, H. Berendsen, *J. Phys. Chem. B* **2000**, *104*, 6380–6388.
[28] S. Marrink, D. Tieleman, A. Mark, *J. Phys. Chem. B* **2000**, *104*, 12165–12173.
[29] C. D. Bruce, M. L. Berkowitz, L. Perera, M. D. Forbes, *J. Phys. Chem. B* **2002**, *106*, 3788–3793.
[30] S. Abel, F.-Y. Dupradeau, E. P. Raman, A. D. MacKerell, Jr., M. Marchi, *J. Phys. Chem. B* **2011**, *115*, 487–499.
[31] J. Lipfert, I. S. Millett, S. Seifert, S. Doniach, *Rev. Sci. Instrum.* **2006**, *77*, 046108.
[32] P. Chen, J. S. Hub, *Biophys. J.* **2014**, *107*, 435–447.
[33] R. Pastor, A. MacKerell, Jr., *J. Phys. Chem. Lett.* **2011**, *2*, 1526–1532.
[34] P. Chen, J. S. Hub, *Biophys. J.* **2015**, *108*, 2573–2584.
[35] T. Soranzo, D. K. Martin, J.-L. Lenormand, E. B. Watkins, *Sci. Rep.* **2017**, *7*, 3399.